SYNTHESIS AND PHOTOLUMINESCENCE OF LiBaBO$_3$: RE^{3+} (RE = Sm & Dy) PHOSPHOR

V.R. Kharabe* and S.P. Puppalwar

Department of Physics, Kamla Nehru Mahavidyalaya, Nagpur 440024, India

A B S T R A C T

A series of Sm and Dy doped LiBaBO$_3$ phosphors were synthesized by solid state reaction method and their photo luminescence (PL) properties were systematically investigated. The synthesized materials were characterized using powder x-ray diffraction pattern (XRD) for confirmation. The microstructures of the phosphors were studied by scanning electron microscope (SEM). The PL emission spectra of Sm^{3+} doped LiBaBO$_3$ were observed at 565 nm and 601 nm in yellow and orange region for 401 nm excitation near UV range. Emission at 565 nm and 601nm are assigned to $^4G_{5/2} \rightarrow {}^6H_{5/2}$ and $^4G_{5/2} \rightarrow {}^6H_{7/2}$ transition of Sm^{3+} ions, respectively. Moreover, PL emission spectra of Dy^{3+} doped LiBaBO$_3$ were observed at 577 and 483 nm in yellow and blue region, respectively on the excitation of 349 nm wavelength. The emission band at 483 nm (blue) corresponds to $^4F_{9/2} \rightarrow {}^6H_{15/2}$ magnetic dipole transition and at 577nm (yellow) corresponding to $^6F_{9/2} \rightarrow {}^6H_{13/2}$ electric dipole transition. The entire characteristics indicate that Dy doped LiBaBO$_3$ phosphors are good candidate for solid state lighting device applications.
Keywords: LiBaBO$_3$XRD, SEM, Photoluminescence, Solid state reaction

1. Introduction

In the past a few decades, rare earth borates have attracted considerable attention due to their practical applications as nonlinear optical (NLO), laser host, and luminescent materials. For example, YAl$_3$(BO$_3$)$_4$, RECa$_4$O(BO$_3$)$_3$ (RE= Y or Gd) [1], La$_2$CaB$_{10}$O$_{19}$ [2], and Na$_3$La$_9$O$_3$(BO$_3$)$_8$ [3] can be used as NLO crystals, Yb:YAl$_3$(BO$_3$)$_4$ and Nd:GdCa$_4$O(BO$_3$)$_3$ [4] are potential self frequency doubling laser crystals, and (Y, Gd)

BO$_3$: Eu^{3+} serves as a good phosphor for plasma display panels (PDPs). In order to search for new functional materials, considerable research should be carried out in the ternary systems like Li$_2$O-BaO-B$_2$O$_3$. The 4f–4f electronic transitions of rare earth ions play an important role in the application such as optical fiber amplifiers, solid-state lasers, planar waveguides and compact microchip lasers [5–7]. In the visible region, the Dy^{3+} ion emits intense yellow (570–600 nm) and blue (470–500 nm) luminescence corresponding to the $^4F_{9/2} \rightarrow {}^6H_{13/2}$ and $^4F_{9/2} \rightarrow {}^6H_{15/2}$ transitions, respectively. Thus, the several Dy^{3+} doped phosphors have been studied to obtain two primary color luminescent materials as well as white-light-emitting material [8, 9].

A suitable red-emitting phosphor for near-UV phosphor converted LEDs should have many potential applications, due to their excellent color rendering index, high color tolerance and high conversion efficiency into visible light [10]. Therefore, it is urgent to find new red phosphors that can be excited by NUV-LED chips for the fabrication of white LEDs. The f-f transition absorption and emission of the crystalline host activated by rare earths ions are of great importance due to their applications as luminescent optical materials emitting in the visible and near IR regions [11–13]. The selection of the rare earth ion as an activator is a key factor for the preparation of luminescence materials. Among the different rare earth ions, the Sm^{3+} ion as an activator is regarded as one of the most popular and efficient doping ions, which can produces intense orange light in the visible wavelength range. Sm^{3+} ions in various hosts show bright emission in orange or red regions because of the transitions from the excited state $^4G_{5/2}$ to the ground state $^6H_{7/2}$ and also to the higher levels ^6H_j (j=7/2, 9/2, and

11/2) and found the application in high density optical storage, temperature sensors, undersea communications, various fluorescent devices, color display and visible solid-state lasers [14, 15]. Selection of suitable host material is also an important factor for the preparation of luminescent materials for different applications. Among the several inorganic host materials, the borate host matrix constitutes as one of the most important luminescence materials, which can produce plenty of crystal field environments imposed on emission contents [16, 17].

On realizing the relevance and importance of these rare earth ions doped borate based phosphors, the present investigation is carried out by the authors. We have been synthesized Dy^{3+} and Sm^{3+} ions doped $LiBaBO_3$ host matrix by a conventional high temperature solid state reaction method in air atmosphere. As far as our knowledge is concerned, the Dy^{3+} and Sm^{3+} doped $LiBaBO_3$ host matrix has not been reported so far. In addition, its structural, thermal, morphological and photoluminescence properties were systematically studied and also analyzed.

2. Experimental

The $LiBa_{1-x}BO_3:xSm^{3+}$ (x=0.1%, 0.5%, 1%, 2%) samples were prepared by modified solid-state reactions in the air atmosphere. $BaCO_3$, H_3BO_3, Li_2CO_3 and Sm_2O_3 (all AR grade and having purity 99.99%) were used as starting materials. The reagents of high purity were weighted in the exact proportions and ground together in an agate mortar for a minimum of half an hour and then transferred to the silica crucible. The samples were first preheated at 550 °C in air for the sufficient diffuse and infiltration of the starting materials, with a soaking time of 3h, for which the samples were firing. Then the preheated mixtures were milled sufficiently again after cooling and then fired at 900 °C for 5h in air with the temperature program 5 °C/min. Then remove sample from furnace after slow cooling having white crystalline floppy powder of Sm^{3+} doped $LiBaBO_3$ phosphors.

The XRD technique was used in order to identify the product and check their crystallinity. The phase composition and phase structure were characterized by X-ray diffraction (XRD) pattern using a PAN-analytical diffractometer with Cu Kα radiation (λ=1.54 A^0) operating at 40Kv, 30mA. The XRD data were collected in a 2θ range from 10 to 80°, with the continuous scan mode. The photoluminescence (PL) emission spectra of the samples were measured at room temperature by using SHIMADZU Spectrofluorophotometer (RF-5301 PC) equipped with a 150W Xenon lamp as the excitation source. The same amount of sample was used in each case. Emission and excitation spectra were recorded using a spectral slit width of 3nm.

3. Results & Discussion

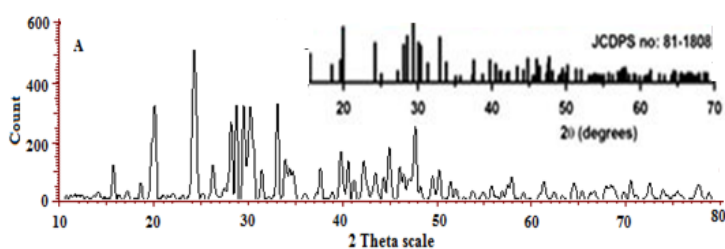### 3.1. *X - ray diffraction pattern and morphology of LiBaBO₃*

Fig.1. X-ray diffraction pattern of LiBaBO₃ (with JCPDS no. 81-1808)   **Fig.3 Crystal structure of LiBaBO₃**
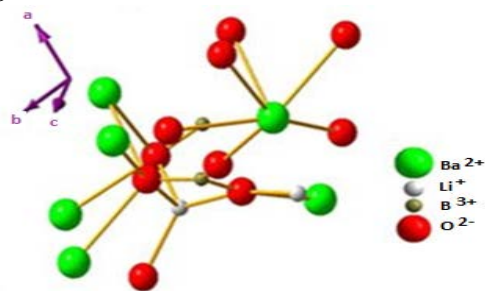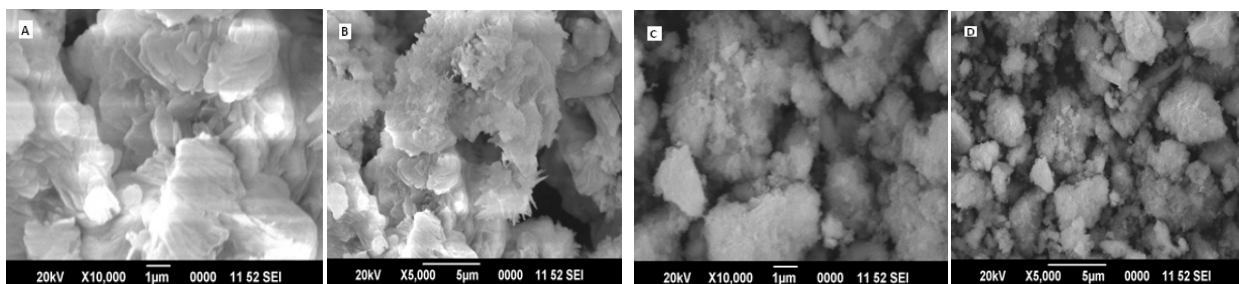
Fig.2. SEM images of LiBaBO$_3$: Dy (A & B) and LiBaBO$_3$: Sm (C & D)

The crystalline formation of the materials is characterized from powder X-ray diffraction (XRD) pattern of LiBaBO$_3$ recorded on Philips P Analytical X'Pert Pro diffractometer at room temperature. The XRD pattern of this material is shown in Fig. 1. The results show the final product was formed in homogeneous and crystalline form. The XRD patterns of LiBaBO$_3$:Sm^{3+} match well with standard 81-1808 JCPDS cards. No second phases are observed indicating that all samples have a single phase and no impurity peaks. The slow scan was performed in 2θ range from 10–80°. The doping of Sm^{3+} has no influence on the crystallizing of the host and Sm^{3+} occupies sites of the alkaline-earth metal ions with similar ion sizes. SEM micrograph images of Sm^{3+} and Dy^{3+} doped LiBaBO$_3$ phosphor are shown in Fig. 2. The images show the particles are polycrystalline with some agglomeration. The crystallites have adhered with each other to form globular clusters of irregular size and shapes. The average size of the crystallites is found to be in the range of 1–2 μm. Fig.3 shows the crystal structure of LiBaBO$_3$.

3.2 Luminescence properties of LiBaBO$_3$:Sm^{3+}
To study the photoluminescence characteristics, the excitation spectrum was recorded for Sm^{3+} doped LiBaBO$_3$ phosphor by monitoring the emission at 601 nm as depicted in Fig. 4(A). Upon this excitation, the photoluminescence emission spectra for different concentrations of Sm^{3+} ions were recorded in the spectral range 500-750 nm. Fig 4(A) presents the excitation

spectra of LiBaBO$_3$: Sm^{3+} phosphor with two dominant excitation bands, which are $^6H_{5/2}$ → $^4H_{7/2}$ and $^6H_{5/2}$ →$^4F_{7/2}$, transitions at 342 nm and 401nm respectively. Fig. 4(B) shows the emission spectra at the excitation wavelength of 401 nm. In the emission spectra of LiBaBO$_3$: Sm^{3+}, the peaks are located at 565 nm ($^4G_{5/2}$ → $^6H_{5/2}$) and 601nm ($^4G_{5/2}$ → $^6H_{7/2}$) respectively. It shows the significant orange emission is due to the $^4G_{5/2}$ → $^6H_{7/2}$ transition at 601 nm splitting into two components and similarly another band at 565 nm also with two components and these split components are probably due to the Stark splitting energy levels though there is another possibility of transitions from $^4F_{3/2}$ and $^4G_{7/2}$ levels to some of the lower levels which could not be ruled out. The energy of the exciting spectral lines is larger than the excitation energy of these levels and they may also be populated by a relaxation process as it happens with the $^4G_{5/2}$ level. The major emission band peaked at 601 nm combined with the other two emission band, leading orange-red light of the LiBaBO$_3$:Sm^{3+} phosphors. In Fig. 4(B), $^4G_{5/2}$ → $^6H_{7/2}$ was stronger than $^4G_{5/2}$ → $^6H_{9/2}$, Therefore, Sm^{3+} mainly took up symmetry center lattice. It is found that the shape and profile for the emission spectra do not vary with the change of the Sm^{3+} doping concentration, but the PL intensity changes greatly. The optimum doping concentration of Sm^{3+} was determined to be 2mol% for obtaining the strongest PL emission intensity.
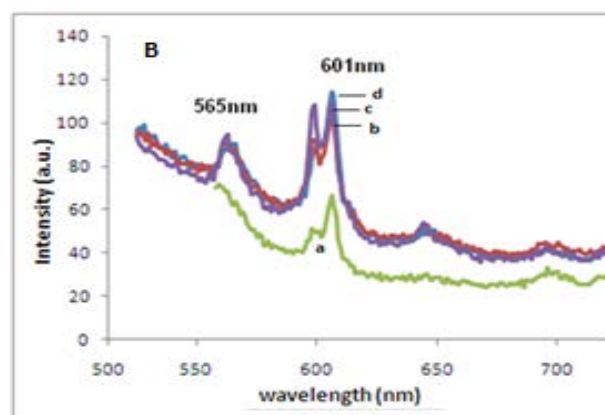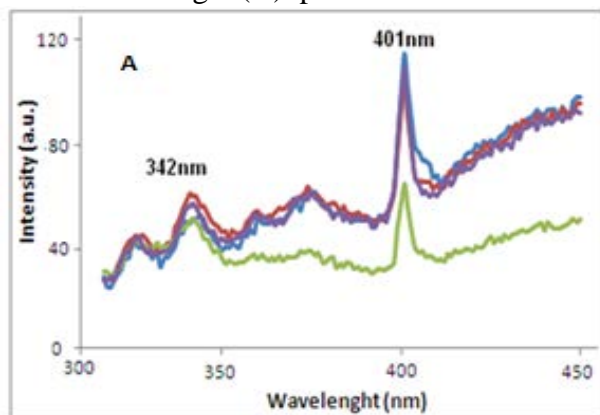
Fig. 4(A) Excitation and (B) Emission spectra of LiBaBO$_3$:Sm^{3+}, for the concentration of Sm^{3+} as (a) 0.1, (b) 0.5, (c) 1 and (d) 2mol%.

3.2 Luminescence properties of LiBaBO$_3$:Dy^{3+}
        The excitation and emission spectra of LiBaBO$_3$:Dy^{3+} for different concentrations are

shown in Fig. 4(A) and (B). The excitation spectrum was measured by monitoring the emission wavelength at 483nm. The excitation

spectrum exhibited three excitation peaks at 348, 364 and 384 nm which are assigned to the electronic transition 4f–4f of the Dy^{3+} ion. Under excitation of 348 nm, the emission spectra of the phosphors show two main emission bands at 483nm (blue) and 578 nm (yellow). The emission bands at 483nm (blue) corresponding to the transition $^4F_{9/2} \rightarrow {}^6H_{15/2}$ magnetic dipole transition, which is much less sensitive to the coordination environment of the host lattice and another emission bands at 578nm (yellow) corresponding to the $^4F_{9/2} \rightarrow {}^6H_{13/2}$ transition belong to the hypersensitive with $\Delta J = 2$ which is forced electric dipole transition being allowed only at low symmetry with no inversion center. The

force electric dipole transition ($^4F_{9/2} \rightarrow {}^6H_{13/2}$) is allowed only when the Dy^{3+} ion is located at the local sites with non-inverted center symmetry. The magnetic dipole transition (blue band) is much more intense than the electric dipole transition (yellow band). The yellow and blue ratio known as the asymmetry ratio of Dy^{3+} ion varies while locating in different host lattices. The optical properties of the material are often influenced by the structure of the matrix and synthesis technique. It is found that the intensity of Dy^{3+} increases with increase of the concentration of Dy^{3+} ion, reaching a maximum value at 2 mol% of Dy^{3+} with no clue of saturation up to the higher concentration in the host lattice.
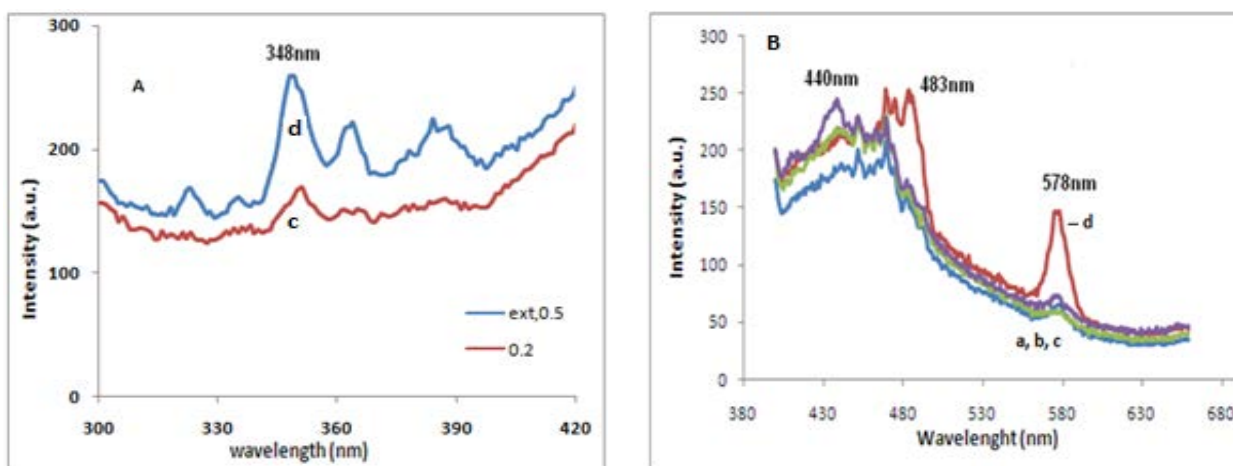

Fig. 5(A) Excitation and (B) Emission spectra of LiBaBO$_3$:Dy^{3+}, for the concentration of Dy^{3+} as (a) 0.2, (b) 0.5, (c) 1 and (d) 2mol%.
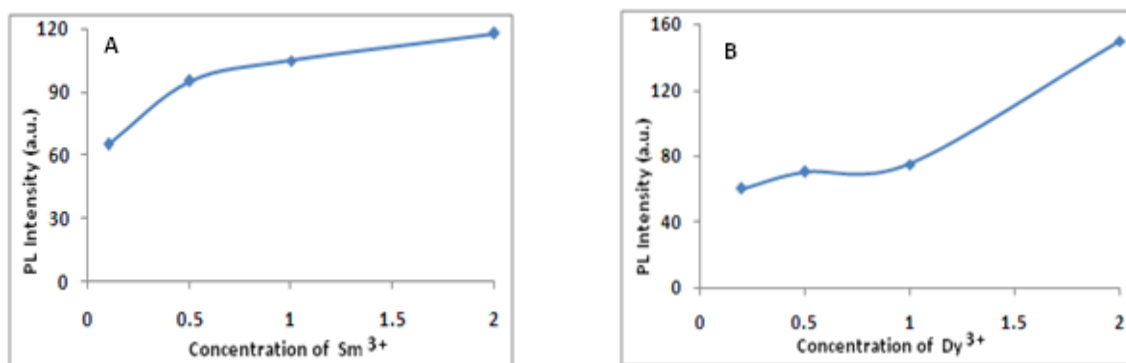

Fig. 6 Effect of concentration of (A) Sm^{3+} and (B) Dy^{3+} ions on PL intensity of LiBaBO$_3$.

4. Conclusion
Sm^{3+} and Dy^{3+} doped LiBaBO$_3$ phosphors have been synthesized by high temperature solid-state reaction method. The photoluminescence properties of LiBaBO$_3$: Sm^{3+} shows that the phosphor emitted orange-red light under excitation of 401nm. The results indicate that LiBaBO$_3$: Sm^{3+} is an efficient orange-red

emitting phosphor and is a suitable material for UV LEDs. The emission spectra of Dy^{3+} LiBaBO$_3$ phosphor show efficient blue (483 nm) and yellow (578 nm) bands at the excitation of 348nm wavelength of UV light. The emission spectra for the Dy^{3+} doped samples are composed of the characteristic emission lines of Dy^{3+} with $^4f_9$ configuration.

The blue emission band is typical emission of Dy^{3+} ion assigned to $^4F_{9/2} \rightarrow {}^6H_{15/2}$ transition and yellow emission is assigned to $^4F_{9/2} \rightarrow {}^6H_{13/2}$ transition. The entire characteristics indicate that Dy doped $LiBaBO_3$ phosphors are good candidate for solid state lighting device applications.

Acknowledgements

REFERENCES

[1] Iwai M, Kobayashi T, Furuya H, Mori Y, Sasaki T, *Crystal Growth and Optical Characterization of Rare-Earth (Re) Calcium Oxyborate $ReCa_4O(BO_3)_3$ (Re=Y or Gd) as New Nonlinear Optical Material* Jpn. J. Appl. Phys 1997; 36; 276-279.

[2] Wu YC, Liu JG, Fu PZ, Wang JX, Yun HY, Wang GF, Chen CT, *A New Lanthanum and Calcium Borate $La_2CaB_{10}O_{19}$* Chem. Mater. 2001; 13; 753-755.

[3] Reshak AH, Auluck S, Kityk IV, Investigation of the *linear and nonlinear optical properties of* $Ag_2In_2SiS_6$ *and* $Ag_2In_2GeS_6$ J. Phys. Condens. Matter 2008; 20; 145209-145215.

[4] Aka G, Brenier A, *Self-frequency conversion in non-linear laser crystals*. Opt. Mater. 2003; 22; 89-94.

[5] Naftaly M, Jha A. *Nd^{3+} doped fluoroaluminate glasses for a 1.3 μm amplifier*. J Appl Phys 2000;87:2098–104.

[6] Machewirth DP, Wei K, Krasteva V, Datta R, Snitzer E, Sigel GH Jr. *Optical characterization of Pr^{3+} and Dy^{3+} doped chalcogenide glasses*. J Non-Cryst Solids 1997; 213: 295–303.

[7] Nogami M, Abe Y. *Properties of sol—gel-derived Al_2O_3-SiO_2 glasses using Eu^{3+} ion fluorescence spectra.* J Non-Cryst Solids 1996; 197: 73–8.

[8] Pekgözlü I, Çakar S. *Photoluminescence properties of $Li_6CaB_3O_{8.5}$:M^{3+} (M^{3+}:Dy and Sm).* J Lumin 2012; 132: 2312–7.

[9] Alajerami YSM, Hashim S, Hassan WMSW, Ramli AT, Kasim A. *Optical and structural properties of lithium sodium borate glasses doped Dy^{3+} ions.* Physica B 2012; 407: 2398–403.

[10] Ye S, Xiao F, Pan YX, Ma YY, Zhang QY, *Phosphors in phosphor-converted white light-emitting diodes: Recent advances in materials, techniques and properties.* Mater. Sci. Eng. 2010; R 71;1-34.

[11] Brown MR, Cox AFJ, Shand WA, Willian JM, *Sensitization of rare earth photoluminescence in II-VI compounds. II. Site sensitive excitation mechanisms in zinc selenide.* J. Phys. C: Solid State Phys. 1972; 5; 502.

[12] Blasse G, *New luminescent materials.* Chem. Mater. 1989; 1; 294-301.

[13] Song E, Zhao W, Zhou G, Dou X, Yi C, Zhou M, *Luminescence properties of red phosphors $Ca_{10}Li(PO_4)_7$:Eu^{3+}*. J. Rare Earths 2011; 29; 440-443.

[14] Li YL, Chang YH, Lin YF, Chang YS, Lin YJ, *Synthesis and luminescent properties of Ln3+ (Eu^{3+}, Sm^{3+}, Dy^{3+}) doped lanthanum aluminum germanate $LaAlGe_2O_7$ phosphors.* J. Alloys Comp. 2007; 439; 367-375.

[15] Setlur AA, Shiang JJ, Happek U, *Eu^{2+}–Mn^{2+} phosphor saturation in 5mm5mm light emitting diode lamps.* Appl. Phys. Lett. 2008; 92; 081104.

[16] Sangen Zhao, Jiyong Yao, Erpan Zhang, Guochun Zhang, Jianxiu Zhang, Peizhen Fu , Yicheng Wu. *Preparation, structure, and photoluminescence properties of new layered borates $KBaRE(B_3O_6)_2$ (RE=Y, Eu, and Tb)* Solid State Sciences 2012; 14; 305-310

[17] Hisanori Yamane, Tetsuya Kawano, Kentaro Fukuda, Takayuki Suehiro, Tsugio Sato. *Preparation, crystal structure and photoluminescence of lithium magnesium manganese borate solid solutions, $LiMg_{1-x}Mn_xBO_3$.* J. Alloys and Compounds. 2012; 512; 223– 229.